Profiling at mRNA, protein and metabolite level reveals alterations in renal amino acid handling and glutathione metabolism in kidney tissue of Pept2-I- mice

Isabelle M. Frey, Isabel Rubio-Aliaga, Anne Siewert, Daniela Sailer, Aleksey Drobyshev, Johannes Beckers, Martin Hrabé de Angelis, Julie Aubert, Avner Bar-Hen, Olivier Fiehn, et al.

Physiol Genomics 28: 301–310, 2007.
First published October 31, 2006; doi:10.1152/physiolgenomics.00193.2006.

Profiling at mRNA, protein, and metabolite levels reveals alterations in renal amino acid handling and glutathione metabolism in kidney tissue of *Pept2*$^{-/-}$ mice

Isabelle M. Frey,[1] Isabel Rubio-Aliaga,[1] Anne Siewert,[1] Daniela Sailer,[1] Aleksey Drobyshev,[2] Johannes Beckers,[2] Martin Hrabé de Angelis,[2] Julie Aubert,[3] Avner Bar Hen,[3] Oliver Fiehn,[4] Hans M. Eichinger,[5] and Hannelore Daniel[1]

[1]*Molecular Nutrition Unit, Technical University of Munich, Freising;* [2]*Institute of Experimental Genetics, GSF, Neuherberg, Germany;* [3]*Applied Mathematics and Informatics Unit INAPG/ENGREF/INRA, Paris, France;* [4]*University of California Davis Genome Center, Davis, California; and* [5]*Laboratory of Bioanalysis, Technical University of Munich, Freising, Germany*

Submitted 1 September 2006; accepted in final form 20 October 2006

Frey IM, Rubio-Aliaga I, Siewert A, Sailer D, Drobyshev A, Beckers J, Hrabé de Angelis M, Aubert J, Bar Hen A, Fiehn O, Eichinger HM, Daniel H. Profiling at mRNA, protein, and metabolite levels reveals alterations in renal amino acid handling and glutathione metabolism in kidney tissue of *Pept2*$^{-/-}$ mice. *Physiol Genomics* 28: 301–310, 2007. First published October 31, 2006; doi:10.1152/physiolgenomics.00193.2006.—PEPT2 is an integral membrane protein in the apical membrane of renal epithelial cells that operates as a rheogenic transporter for di- and tripeptides and structurally related drugs. Its prime role is thought to be the reabsorption of filtered di- and tripeptides contributing to amino acid homeostasis. To elucidate the role of PEPT2 in renal amino acid metabolism we submitted kidney tissues of wild-type and a *Pept2*$^{-/-}$ mouse line to a comprehensive transcriptome, proteome and metabolome profiling and analyzed urinary amino acids and dipeptides. cDNA microarray analysis identified 147 differentially expressed transcripts in transporter-deficient animals, and proteome analysis by 2D-PAGE and MALDI-TOF-MS identified 37 differentially expressed proteins. Metabolite profiling by GC-MS revealed predominantly altered concentrations of amino acids and derivatives. Urinary excretion of amino acids demonstrated increased glycine and cysteine/cystine concentrations and dipeptides in urine were assessed by amino acid analysis of urine samples before and after in vitro dipeptidase digestion. Dipeptides constituted a noticeable fraction of urinary amino acids in *Pept2*$^{-/-}$ animals, only, and dipeptide-bound glycine and cystine were selectively increased in *Pept2*$^{-/-}$ urine samples. These findings were confirmed by a drastically increased excretion of cysteinylglycine (cys-gly). Urinary loss of cys-gly together with lower concentrations of cysteine, glycine, and oxoproline in kidney tissue and altered expression of mRNA and proteins involved in glutathione (GSH) metabolism suggests that PEPT2 is predominantly a system for reabsorption of cys-gly originating from GSH break-down, thus contributing to resynthesis of GSH.

PEPT2; peptide transport; glutathione metabolism; pathway analysis

CELLULAR UPTAKE OF DI- AND TRIPEPTIDES is mediated in prokaryotes and eukaryotes by membrane proteins of the peptide transporter (PTR) family (36). The peptide transporters PEPT1 (Slc15a1) and PEPT2 (Slc15a2) and the peptide-histidine transporters PHT1 (Slc15a4) and PHT2 (Slc15a3) form the two subgroups of proteins belonging to the PTR family in mammals. The PHT proteins appear to transport primarily histidine but also selected di- and tripeptides. PHT1 is found in brain, retina, skeletal muscle, and kidney (7, 41), while PHT2 is expressed primarily in the lymphatic system but also in the lung and placenta (33).

In contrast to the PHT proteins, PEPT1 and PEPT2 have been well characterized since their cloning a decade ago (5, 6, 13, 21) with a number of recent reviews summarizing current knowledge on structure and mode of transport function (12, 15, 30). A unique feature is their ability to transport a huge range of substrates. Besides all possible di- and tripeptides independent of sequence, size, charge, or polarity, peptidomimetics such as β-lactam antibiotics, angiotensin I converting enzyme inhibitors, and prodrugs like Val-Acyclovir are transported as well. Transport is stereoselective and occurs along an inwardly directed electrochemical proton gradient. Both transporters are mainly expressed in apical membranes of epithelial cells. PEPT1 is the low affinity system with substrate affinities in the millimolar range but with high transport capacity, whereas PEPT2 is characterized by high substrate affinities (micromolar range) for the same substrates but with a lower transport capacity. The main function of PEPT1 lies in the absorption of large quantities of dietary di- and tripeptides in the small intestine. Its importance for protein nutrition, growth, and development has for example been demonstrated in a *Caenorhabditis elegans* model lacking the ortholog *pep2* gene (23). PEPT1 is also expressed in kidney tubules and the bile duct. In contrast, PEPT2 is found in numerous organs with highest expression levels in kidney and lower expression in the nervous system, lung, mammary gland, and choroid plexus. Expression in glial cells in the enteric nervous system of the gut has also been shown recently (32). Although well understood in function at the molecular level, the physiological role of PEPT2 in the different organs in which it is expressed has not been well defined as yet.

In the kidney, peptides and amino acids are reabsorbed from the glomerular filtrate by the activities of peptide transporters and amino acid transporters acting in parallel in the apical membrane of tubular epithelial cells (for review see Refs. 1, 26). The localization of PEPT1 in the S1 segment of the proximal tubule and PEPT2 in the S2 and S3 segment has led to the concept that the high capacity transporter PEPT1 is responsible for the reabsorption of bulk quantities of peptides in the more proximal part, whereas PEPT2 functions as the

Address for reprint requests and other correspondence: H. Daniel, Molecular Nutrition Unit, Technical Univ. of Munich, Am Forum 5, D-85350 Freising, Germany (e-mail: daniel@wzw.tum.de).

high affinity transporter, acting in the more distal parts of the proximal tubule taking care of the remaining luminal substrates. Yet early studies in rabbit brush border membrane vesicles already indicated that mainly a high affinity system (PEPT2) is responsible for the bulk uptake of di- and tripeptides in the tubule (20).

To assess the role of PEPT2 in renal peptide reabsorption a mouse model that lacks a functional PEPT2 protein has been generated (31). Animals were proven to have severely impaired renal reabsorption of radiolabeled and fluorogenic model dipeptides, confirming the notion PEPT2 plays the prominent role in renal dipeptide handling. Moreover, lack of PEPT2 did not lead to any compensatory upregulation of either PEPT1 or PHT1 transporters in kidney, neither at the mRNA nor protein levels. Recent clearance studies with the dipeptide glycyl-sarcosine in *Pept2*$^{-/-}$ and wild-type mice established that PEPT2 indeed accounts for 86% of overall renal peptide reabsorption (25). Mice lacking the peptide transporter PEPT2 nevertheless display only very little phenotypic alterations (14, 35). To assess to which extent this lack of a prominent phenotype in *Pept2*$^{-/-}$ mice is caused by biological redundancy, a comprehensive analysis of mRNA, protein, and metabolite levels in the same kidney tissue samples of transporter-deficient and control animals was performed in combination with the assessment of urinary losses of amino acids and dipeptides.

MATERIALS AND METHODS

Animals and Sample Collection

The generation of the PEPT2-deficient mice (Slc15a2^{tm1Dan}) by targeted disruption of the *Pept2* gene has been reported previously (31), and animals were bred on a mixed genetic background of C57/BL6 and 129Sv. Homozygous animals of the *Pept2*$^{+/-}$ line were mated to yield litters of entirely *Pept2*$^{+/+}$ or *Pept2*$^{-/-}$ pups for the experiments. Animals were maintained at 22 ± 2°C and a 12–12 h light-dark cycle with access to tap water and a standard rodent diet (Altromin, 1320; Detmold, Germany) ad libitum. The genotype of an animal was identified by PCR screening with a primer pair directed against the first intron of the *Pept2* wild-type allele (forward primer: 5′-cca ctg aaa ctg aca ccc ac-3′, reverse primer: 5′-gct ctg cac aca agg gaa ac-3′), which is replaced in the targeted allele, and with a primer pair directed against the lacZ cassette that is inserted in the targeted allele (forward primer: 5′-cag gat atg tgg cgg at gag-3′, reverse primer: 5′-gtt caa cca ccg cac gat ag-3′).

Tissue sampling for transcriptome, proteome, and metabolome analysis. Kidneys were removed after cervical dislocation from five *Pept2*$^{-/-}$ and five *Pept2*$^{+/+}$ mice (all male) at the age of 88 ± 2 days between 8 and 10 AM and snap-frozen in liquid nitrogen. One of the kidneys of each animal was used for isolation of total RNA, and the other kidney was homogenized and aliquots were used for extraction of proteins and metabolites.

Sample collection for analysis of amino acids and dipeptides in urine and expression of genes involved in glutathione (GSH) metabolism. Pept2$^{+/+}$ and *Pept2*$^{-/-}$ animals (all male, $n = 10–12$) were fed a semisynthetic purified diet formulated according to AIN-93G. At the age of 8 wk, mice were placed in metabolic cages that allowed collection of urine and monitoring of food and water consumption. For 18 days mice had free access to food and tap water ad libitum. Body weight and consumption of food and water were monitored daily. On *days 19–23* mice were placed in clean metabolic cages, and food was removed for the 12 h during the dark phase to allow for urine collection without any contamination of urine by food. Containers for urine collection were cooled, and 10 μl of 10% thymol in isopropanol were added to avoid bacterial degradation of metabolites. Urine samples were stored at −20°C until analyzed for free and dipeptide-bound amino acids. Mice were killed by cervical dislocation on *day 24* between 8 and 10 AM after the last urine collection period. Kidneys were removed and immediately snap-frozen in liquid nitrogen.

Sample collection for determination of cysteinyl-glycine in spot urine samples and GSH levels in kidney tissue. Spot urine samples of 10 animals per sex and genotype were collected at the age of 12 wk on 5 consecutive days between 9 and 10 AM by mild pressure on the lower abdomen. Samples were immediately frozen and stored at −20°C until analysis. Kidney samples for determination of GSH were quickly removed after cervical dislocation and immediately snap-frozen in liquid nitrogen. Kidneys of 8–10 animals per genotype were collected at the age of 14 wk. Individual kidneys were homogenized in a mortar under liquid nitrogen, and 25 mg of tissue samples were extracted with 5% sulfosalicylic acid by ultra sonification (30 strokes, low amplitude) on ice. Samples were centrifuged, and the supernatant was neutralized with 2 M $KHCO_3$ and stored at −20°C until analyzed. All procedures applied throughout this study were conducted according to the German guidelines for animal care and approved by the state ethics committee under reference number 209.1/211-2531-41/03.

Isolation of Total RNA, Reverse Transcription, and Fluorescent Labeling

Individual kidneys were transferred into buffer containing chaotropic salt (RLT buffer; Qiagen, Hilden, Germany) and immediately homogenized with a Polytron homogenizer. Total RNA was obtained according to the manufacturer's protocols using RNeasy Midi kits (Qiagen). For each cDNA array, 20 μg of total RNA were used for reverse transcription and indirect labeling with the fluorescent dyes Cy3 or Cy5 (Amersham Biosciences, Freiburg, Germany) according to the TIGR protocol (18).

cDNA Array Expression Profiling

cDNA arrays employed and procedures for hybridization have been described previously (34). Briefly, probes were PCR amplified from the 20,000 (20k) mouse arrayTAG clone set (LION Bioscience, Heidelberg, Germany), dissolved in 3× SSC, and spotted on aldehyde-coated slides (CEL Associates, Pearland, TX) using the Microgrid TAS II spotter (Biorobotics Genomic Solutions, Huntingdon, UK) with Stealth SMP3 pins (Telechem, Sunnyvale, CA). Spotted slides were rehydrated, blocked, denatured, and dried. Labeled cDNA was dissolved in 30 μl of hybridization buffer (6× SSC, 0.5% SDS, fivefold Denhardt solution, and 50% formamide) and mixed with 30 μl of reference cDNA solution labeled with the second dye. The hybridization mixture was placed on a prehybridized microarray and hybridized at 42°C for 18–20 h. After hybridization, microarrays were immersed in 40 ml of 3× SSC and then successively washed in 40 ml of 3× SSC, 40 ml of 1× SSC, and 40 ml of 0.25× SSC at room temperature and centrifuged for drying. Dried slides were scanned with a GenePix 4000A microarray scanner, and the images were analyzed using the GenePix Pro 3.0 image processing software (Axon Instruments). cDNA of each of the 5 *Pept2*$^{-/-}$ mice was hybridized individually against an equimolar pool of the five *Pept2*$^{+/+}$ animals. Additionally cDNA samples of four of the wild-type mice were hybridized individually against cDNA of the fifth wild-type mouse to account for biological variation within the control animals. Each hybridization was repeated four times including two dye swaps.

Microarray Data Analysis

Data were formatted according to MIAME standards and submitted to the Gene Expression Omnibus (GEO) database as series GSE1585 and GSE1586. For further analysis, intensity-dependent normalization was performed with the LOESS (42) procedure followed by subtraction of the log-ratio median calculated over the values for an entire

block from each individual log-ratio using the *anapuce* package of R. Differential analysis was performed with the *varmixt* package of R (10). Variability of the variances was computed according to the number of available observations. A double-sided, unpaired *t*-test was computed for each gene between both conditions (10). The variance was split between subgroups of genes with homogeneous variance. The multiplicity of test was taken into account with false discovery rate corrections (4).

Real-time Reverse Transcription PCR

Changes in transcript levels of genes identified as regulated in cDNA microarray analysis were validated exemplarily by real-time reverse transcription PCR analysis of Eaf2 and RNase4 with the same RNA samples used for the microarray analysis and with RNA from kidney tissue samples of mice from the metabolic study. Total RNA of kidney tissues of five mice per genotype was isolated individually with the RNeasy Mini kit (Qiagen) according to the manufacturers protocol. Of each individual kidney 1 μg of total RNA was transcribed into cDNA with MMLV-RT (Promega) and random hexamers (Fermentas). Quantitative real-time PCR (qPCR) was performed on a LightCycler (Roche, Penzberg, Germany) with 3.3 ng of cDNA per PCR reaction and the FastStart SYBR Green Kit (Roche, Mannheim, Germany). Cycle parameters were annealing at 62°C for 10 s, extension at 72°C for 20 s, and melting at 95°C for 15 s. Specificity of PCR products was controlled by melting curve analysis and by agarose gel electrophoresis. Primers were designed using the Primer3 web interface (http://www-genome.wi.mit.edu/cgi-bin/primer/primer3_www.cgi) except primers for hypoxanthine phosphoribosyltransferase (Hprt) (ID 45 in RTPrimerDB) (28) and succinate dehydrogenase complex, subunit A (Sdha) [PrimerBank ID15030102a3 (38)]: ribonuclease, RNase A family 4 (Rnase4) (forward primer 5′-CTTTCTCCCCTTGGATGGGATG-3′, reverse primer 5′-TAGGCGAGTTGTCATTGCCTG-3′), ELL associated factor 2 (Eaf2) (forward primer 5′-CGGAGCACCCTAGCATGTC-3′, reverse primer 5′-CTGTCGCTTTCTGACTC-3′), (glyceraldehyde-triphosphate dehydrogenase) (Gapdh) (5′-ATCCCAGAGCTGAACG-3′, GAAGTCGCAGGAGACA-3′), Hprt (5′-CCTAAGATGAGCGCAAGTTGAA-3′, 5′-CCACAGGACTAGAACACCTGCTAA-3′), Sdha (5′-TCCTGCCTCTGTGGTTGAG-3′, 5′-AGCAACACCGATGAGCCTG-3′). For relative quantification the geometric mean of crossing point (CP) values of the three housekeeping genes Gapdh, Hprt, and Sdha was calculated for each sample as described in (29). This best-keeper index was used as CP of the reference gene to calculate mean normalized expression (MNE) values for each sample as described in Ref. 24.

Real-time PCR analysis was also performed for a subset of genes from pathways of glutathione metabolism with kidney tissue samples of mice from the metabolic study. qPCR cycle parameters were annealing at 62°C for 10 s, extension at 72°C for 20 s, and melting at 95°C for 15 s. Primers were designed by the LightCycler Probe Design software vers. 1.0 (Roche, Penzberg, Germany): glutamylcysteine ligase catalytic subunit (Gclc) (5′-AGGATCAGTAAGTCTCGG-3′, 5′-GTGAGCAGTACCACGAATA-3′), glutamylcysteine ligase modifier subunit (Gclm) (5′-GGTACTCGGTCATCGTG-3′, 5′-GCTTCTTGTAAGGCGG-3′), glutathione synthetase (Gss) (5′-ACGACTATACTGCCCG-3′, 5′-GTAGCACCACCGCATT-3′), γ-glutamyl-transferase (Ggt1) (5′-AGGAGAGACGGTGACT-3′, 5′-GGCATAGGCAAACCGA-3′), glutathione reductase 1 (Gsr) (5′-TTCGACGGGACCCAAA-3′, 5′-ACATCGGGGTAAAGGC-3′), cystathionine gamma-lyase (Cth) (5′-TTGCTAGAGGCAGCGA-3′, 5′-AAGCCGACTATTGAGGT-3′). Relative quantification was performed as described above.

Sample Preparation for Two-dimensional Gel Electrophoresis

Individual kidneys were homogenized in a mortar under liquid nitrogen, 50 mg of tissue were transferred into 500 μl of lysis buffer [7 M urea, 2 M thiourea, 2% CHAPS, 1% dithiothreitol (DTT), 2% Pharmalyte, Complete Mini proteinase inhibitor], and homogenization was achieved by ultrasonification (30 strokes, low amplitude) on ice. Lysed tissue samples were centrifuged for 30 min at 100 000 *g* at 4°C, and protein concentrations were determined by a modified Bradford assay (Bio-Rad protein assay). Protein extracts were dialyzed with the Plusone Mini Dialysis Kit (Amersham) against a modified lysis buffer (7 M urea, 2 M thiourea, 1% DTT) and stored at −80°C until analyzed.

Two-dimensional Gel Electrophoresis

Two-dimensional gel electrophoresis (2D-PAGE) was performed as described by Fuchs et al. (15). In brief, 300 μg of protein were loaded by cup-loading, and isoelectric focusing was performed on 18-cm immobilized pH gradient strips (pH 3–10; Amersham Biosciences, Freiburg, Germany) using an Amersham IPGPhor unit. We ran 12.5% SDS-polyacrylamide gels on an Amersham Bisosciences Ettan-Dalt II system in the second dimension. Gels were fixed and subsequently stained with Coomassie blue (CBB G-250; Serva, Heidelberg, Germany). Two gels were performed for every individual animal. Gels were scanned and analyzed using the ProteomWeaver software (Definiens Imaging, Munich, Germany), which combined the spot detection with automatic background subtraction and normalization of the spot volumes. Spots differing significantly ($P < 0.05$, double sided, unpaired Student's *t*-test) in density were picked for matrix-assisted laser desorption/ionization-time of flight-mass spectrometry (MALDI-TOF-MS) analysis.

Tryptic Digestion of Protein Spots and Peptide Mass Fingerprinting by MALDI-TOF-MS

All methods applied here have been described in detail by Fuchs et al. (15). In brief, CBB-stained spots were picked, destained, and digested in gel with sequencing grade modified trypsin (Promega). The resulting peptide fragment extracts were analyzed by MALDI-TOF-MS with an Autoflex mass spectrometer (Bruker Daltonics, Leipzig, Germany). Proteins were identified with the Mascot Server 1.9 (Bruker Daltonics) based on mass searches with mouse sequences only. The criteria for positive identification of proteins were set as follows: *1*) a minimum score of 63, *2*) mass accuracy of ± 0.01%, and *3*) at least twofold analysis from four independent gels.

Metabolite Profiling by Gas Chromatography-Time of Flight-Mass Spectrometry

Metabolite levels in kidney tissue were analyzed as described in (39) with minor modifications. Briefly, individual kidneys were homogenized in a mortar under liquid nitrogen and 5 mg of tissue were extracted with a solvent mixture of methanol-chloroform-water 2.5:1:1 vol/vol/vol kept at −20°C. Further fractionation of the extracts and derivatization of metabolites were performed as described previously (40). Gas chromatography-time of flight-mass spectrometry (GC-TOF-MS) analysis was performed using a HP5890 gas chromatograph with standard liners containing glass wool in a splitless mode at 230°C injector temperature with a liner exchange for every 50 samples. The GC was operated at constant flow of 1 ml/min helium on a 30-m, 0.25-mm inner diameter, 0.25-μm RTX-5 column with a 10-m integrated precolumn. The temperature gradient started at 80°C, was held isocratic for 2 min, and subsequently ramped at 15°C/min to a final temperature of 330°C, which was held for 6 min. Data were acquired on a Pegasus II TOF mass spectrometer (LECO, St. Joseph, MI) and CHROMATOF 1.61 software at 20 s^{-1} from m/z 85–500, R = 1.70 kV electron impact and autotuning with reference gas CF 43. Samples were compared against reference chromatograms that had a maximum of detectable peaks at signal/noise >20. For identification and alignment, peaks were matched against a customized reference spectrum database, based on retention indexes and mass spectral similarities. Relative quantification was performed on ion traces chosen by optimal selectivity from coeluting compounds. Artifact

peaks resulting from column bleeding, phthalates, and polysiloxanes were removed. All data were normalized to tissue fresh weight and to internal references (ribitol and nonadecanoic acid methyl ester). Data were log-transformed, resulting in more Gaussian-type distributions. Differences between transporter-deficient and control animals were analyzed by principal component analysis (PCA) and partial least squares discriminant analysis (PLS-DA) after centering and unit variance (UV) scaling of the complete data set (identified and unidentified compounds) with SIGMA P (Umetrics, Umeå, Sweden). PLS-DA was cross-validated by leaving out 20% of the samples, calculating a new model on the remaining samples and predicting the class membership of the left out samples. This process was repeated five times.

Analysis of Urinary Free and Dipeptide-bound Amino Acids

Urine samples of the metabolic study (n = 10–12 per genotype) were prepared for amino acid analysis in parallel with or without digestion by renal membrane dipeptidase (EC 3.4.19.3) that was kindly provided by Dr. N. Hooper (University of Leeds, Leeds, UK). In vitro hydrolysis of urinary dipeptides was performed by incubation of 200 μl of urine with 500 ng of dipeptidase for 30 min at 37°C. Amino acids were analyzed by ion-exchange chromatography with a Biotronic LC3000 amino acid analyzer (Eppendorf, Hamburg, Germany) employing a lithium borate-acetate buffer system and ninhydrin postcolumn detection. Data were used if duplicate analysis indicated reliable quantification resulting in analysis of an average of 6–12 mice per genotype depending on the amino acid detected. The detection limit of the amino acids (defined as signal-to-noise ratio $>$ 5) was ~1 μmol/l, and the recovery of amino acids added at known concentrations to urine samples varied between 93 and 110%. Creatinine was analyzed with an Olympus AU400 autoanalyzer (Hamburg, Germany) with adapted reagents from Olympus and Roche (Mannheim, Germany), and data on urinary amino acids are expressed in mmol/mol creatinine.

HPLC-based Determination of Cysteinyl-Glycine in Urine and GSH in Kidney Tissue

Cysteinyl-Glycine (cys-gly) in urine and GSH in tissue extracts were determined by HPLC after derivatization with monobromobimane according to the method of Pastore et al. (27) with slight modifications. In brief, 26 μl of sample were mixed with 26 μl of 4 M $NaBH_4$ (dissolved in a solution of 333 ml/l DMSO and 66 mmol/l NaOH in water), 18.2 μl EDTA (2 mmol/l)-DTT (2 mmol/l), 5.2 μl 1-Octanol, 10.4 μl HCl (1.8 mol/l), and 26 μl HCl (0.1 mol/l)-DTT 0.1 (mmol/l). After incubation for 3 min at room temperature, 39 μl of N-ethylmorpholine buffer (2 mol/l, pH 8.0), 7.8 μl monobromobimane (25 mmol/l in 1:1 acetonitrile/H_2O), and 156 μl bidistilled H_2O were added. After incubation for 4 min at room temperature, the reaction was stopped with 15.6 μl of acetic acid. Samples were analyzed on a Merck Hitachi HPLC system consisting of an L-5000 LC-Controller, a 655–11 Liquid Chromatograph, a F-1050 Fluorescence Spectrophotometer, and a D-2000 Chromato-Integrator. We injected 50 μl of the derivatized sample onto a 150 × 4.6 mm Hypersil-ODS column (3 μm particle size), 30°C column temperature, equilibrated with *eluent 1* [96% *buffer A*: ammonium nitrate (30 mmol/l), ammonium formate (40 mmol/l) pH 3,55; 4% acetonitrile] and 3% *eluent 2* (80% acetonitrile, 20% *buffer A*). The derivatized thiols were eluted with a gradient of *eluent 2* (0–5 min, 3–5% *eluent 2*; 5–10 min, 5–6% *eluent 2*; 10–12 min, 6–14% *eluent 2*; 12–16 min, 14–100% *eluent 2*; 17–19 min, 100–3% *eluent 2*; 19–23 min, 3% *eluent 2*) at a flow rate of 1.5 ml/min. Fluorescence of the bromobimane adducts was determined at an excitation wavelength of 390 nm and an emission wavelength of 478 nm. The detection limit of thiols was ~200 nmol/l, and the recovery of added cys-gly or GSH varied between 102 and 114%.

Statistical Analysis

Statistical analyses of amino acids in urine, MNE values of differentially expressed genes and thiols in urine and tissues were performed by SPSS version 12.0.1. The level of statistical significance was set at $P < 0.05$. Values are given as means ± SE. In case that Gaussian distribution was not given, nonparametric tests were applied.

RESULTS

Transcriptome Analysis of Kidney Samples by cDNA Microarrays

Differential gene expression in kidneys of *Pept2*$^{-/-}$ and *Pept2*$^{+/+}$ animals was assessed with 20k cDNA microarrays (34); 159 genes did show significantly altered mRNA levels in the transporter-deficient animals. As 12 of these genes were represented by two cDNA probes on the array, the total number of unique regulated transcripts was 147, with higher mRNA abundance for 79 genes and lower mRNA levels for 68 genes in *Pept2*$^{-/-}$mice. *Rnase4* and *Eaf2* were chosen for validation of microarray results by qPCR. Differential expression of *Rnase4* and *Eaf2* could be verified in the RNA samples that had been used for the microarray analysis as well as in kidney tissue of mice of the metabolic study. *Rnase4* was consistently found upregulated (with a mean change in *Pept2*$^{-/-}$ mice as determined by qPCR of 5.4-fold and 3.0-fold in samples used for the microarray analysis and samples from animals of the metabolic study, respectively). *Eaf2* was always found downregulated (mean change in *Pept2*$^{-/-}$ mice as determined by qPCR of −1.6-fold and −1.8-fold in samples used for the microarray analysis and from animals of the metabolic study, respectively). These consistent changes in expression level of the target genes even under different housing and feeding conditions confirm that regulation of *Rnase4* and *Eaf2* expression is indeed due to loss of the peptide transporter PEPT2. A complete list of altered mRNA species identified by cDNA microarray analysis is provided in Table S. 1 in the supplementary data set. (The online version of this article contains supplemental data.)

2D-PAGE and MALDI-TOF Analysis of Kidney Proteome

Table 1 displays proteins with significantly altered levels in kidney tissues of transporter-deficient animals. On average, 350 proteins could be resolved by 2D-PAGE analysis in a gel of which 37 showed major changes; 18 of these proteins could be identified by MALDI-TOF-MS, and 12 of the identified proteins with altered abundance in transporter-deficient animals were represented by a probe on the cDNA microarray. Yet only glutathione transferase mu1 (Gstm1) showed a parallel increase in mRNA abundance and protein. For none of the other identified proteins a regulation at transcript level was observed.

Metabolite Profiling by GC-TOF-MS

On average, 746 metabolite peaks could be detected in kidney tissue extracts, of which 139 could be assigned to known compounds. Multivariate data analysis was applied to the dataset to analyze whether a characteristic metabolic fingerprint differentiates between samples of knockout and wild-type animals. PCA revealed that 29% of the total variance of

Table 1. *Changes in protein level in kidney tissue of PEPT2-deficient animals*

Protein	Gene Symbol	Function	Measured pI/MW	Theoretical pI/MW	% Sequence Coverage	Ratio $Pept2^{-/-}/Pept2^{+/+}$	*P* (*t*-test)	ID*	mRNA Δ-fold Change in $Pept2^{-/-}$
Proteins with higher steady-state levels in kidneys of $Pept2^{-/-}$ mice									
Albumin	*Alb1*	plasmatic transport	6.51/52.1	5.62/68.7	36	2.83	0.024	MG-8-118e21	
Sepiapterin reductase	*Spr*	metabolism	5.81/31.1	5.78/27.9	33	2.63	0.039	MG-15-219m12	
Epoxide hydrolase	*Ephx2*	detoxification	6.10/61.3	5.86/52.6	34	2.22	0.016	MG-15-146f14	
Isocitrate dehydrogenase 3 (NAD+) beta	*Idh3b*	metabolism	8.56/45.7	8.76/42.2	48	2.14	0.026		
Glycine amidinotransferase	*Gatm*	amino acid metabolism	6.91/51.8	8.00/48.3	29	2.13	0.004		
3-Hydroxyantranilate 3,4-dioxygenase	*Haao*	metabolism	6.70/36.7	6.09/32.8	46	2.11	0.001	MG-12-248l12	
Methionine sulfoxide reductase A	*Msra*	protein metabolism	7.32/28.8	8.60/26.0	53	2.07	0.023	MG-6-46m3	
Glutathione transferase mu1	*Gstm1*	detoxification	9.03/30.0	7.92/25.8	33	2.07	0.036	MG-3-22g11	1.16
Pyruvate kinase M2 isozyme	*Pkm2*	metabolism	8.00/60.8	7.38/57.8	25	1.87	0.022	MG-6-48g14	
Phosphotriesterase related	*Pter*	metabolism	6.61/44.4	5.97/39.2	24	1.66	0.002		
3-Oxoacid CoA transferase	*Oxct1*	lipid metabolism	8.22/58.6	8.86/56.0	30	1.65	0.029	MG-15-75h11	
Nit protein 2	*Nit2*	metabolism	6.66/34.6	6.78/30.5	61	1.54	0.006	MG-12-178b2	
Dihydrolipoamide transacylase precursor	*Dbt*	metabolism	6.56/55.5	8.79/53.2	29	1.51	0.007		
Quinolinate phosphoribosyltransferase	*Qprt*	nucleotide biosynthesis	6.53/41.1	6.24/27.8	24	1.51	0.011		
Proteins with lower steady-state levels in kidneys of $Pept2^{-/-}$ mice									
Homogentisate dioxigenase	*Hgd*	amino acid metabolism	7.06/53.6	6.86/50.0	31	0.49	0.008	MG-12-23i12	
Coproporphyrinogen oxidase	*Cpox*	cellular biosynthesis	7.95/42.4	8.00/49.7	55	0.57	0.031		
Laminin receptor 1	*Lamr1*	cytoskeletal protein	4.12/43.1	4.77/32.6	35	0.60	0.027	MG-12-147c15	
Aconitate hydratase	*Aco1*	metabolism	7.89/97.0	7.10/98.2	22	0.65	0.019	MG-12-136j1	

*Lion Biosciences Probe ID for proteins that are represented by a cDNA probe on the cDNA microarray.

the data set was accounted for by the first principal component and that an additional 18% of the overall variance was explained by the second principal component. Yet only partial separation between samples of different genotypes could be observed. Analysis for metabolites that contribute most to discrimination between genotypes by PLS-DA provided a clear separation between genotypes. PLS-DA was cross-validated by leaving out 20% of the samples, calculating a new model on the remaining samples, and predicting the class membership (knockout or wild type) of the left-out samples. This process was repeated five times. Class membership was predicted correctly by these training models for 9 out of 10 samples. Identified metabolites that contributed most to discrimination between genotypes are listed in Table 2 and revealed primarily lower levels of amino acids and amino acid derivatives in kidney samples of transporter-deficient animals.

Table 2. *Changes in metabolite concentrations in kidney tissue of $Pept2^{-/-}$ mice*

Variable Importance List*	Ratio KO/WT†
Oxoproline	0.6
Putrescine	0.5
Cysteine	0.8
Tryptophane	0.7
Threonine	0.8
Pipecolic acid	0.8
Glycolic acid	0.7
Hydroxyproline	0.8
Glutamate	1.1
Pyruvate	0.5
Azelaic acid	0.7
Galactonic acid	0.7
Proline	0.8
Phosphoethanolamine	1.3
Lysine	0.8
Glycine	0.9
Alanine	0.7
Threonic acid	0.9
Tyrosine	0.8
Serine	0.9

Identified and unidentified compounds analyzed by gas chromatography-time of flight-mass spectrometry were examined by partial least squares discriminant analysis to identify compounds that contribute most to differentiation between knockout (KO) and wild-type (WT) kidney tissue. *Identified metabolites that contributed most to class prediction ($Pept2^{-/-}/Pept2^{+/+}$); †Ratio of mean concentrations levels, $n = 5$ per genotype.

Urinary Excretion of Amino Acids and Dipeptides

Analysis of urine samples covered free amino acids and dipeptide-bound amino acids as determined by increases in free amino acids after in vitro hydrolysis of urine samples with a nonspecific dipeptidase. Values for free amino acids and amino acids after dipeptidase hydrolysis are given in Table 3. Urine in vitro hydrolysis led to a significant increase in amino acid concentrations in the case of glycine and cystine in the transporter deficient animals, only, resulting in a significant differ-

Table 3. *Free and dipeptide bound amino acids in urine*

		Free Amino Acids, mmol/mol creatinine		Amino Acids After Dipeptidase Digestion, mmol/mol creatinine	
	n	+/+	−/−	+/+	−/−
Threonine	8–10	92.2±7.77	90.8±10.8	92.8±7.50	87.0±7.14
Serine	7–10	43.5±5.48	52.9±16.3	44.5±6.82	47.6±9.71
Glycine	9–12	207.9±15.1	253.1±45.8*	245.2±18.8†	462.1±64.2*†
Alanine	9–10	88.8±14.7	107.0±23.7	91.7±14.2	96.9±10.8
Cystine	8–12	73.1±9.27	68.0±7.20**	85.0±11.1†	161.0±22.4**†
Methionine	5–11	62.0±6.55	61.4±6.86	61.5±6.71	56.0±6.39
Isoleucine	5–11	47.6±7.51	53.9±12.6	47.9±6.48	50.2±7.40
Leucine	6–11	76.6±14.6	88.9±15.0	75.1±13.6	85.5±9.47

Values are means ± SE. All data analyzed by Kruskal-Wallis and Mann-Whitney *U*-test with Bonferroni correction for differences in respect to genotype, protein content of the diet, and analysis previous to and after dipeptidase digestion. †Significant differences between genotypes (†$P < 0.05$); *significant differences between free amino acids and amino acids after dipeptidase digestion (*$P < 0.05$, **$P < 0.01$).

ence of dipeptide-bound cystine and glycine between *Pept2*$^{-/-}$ and *Pept2*$^{+/+}$ mice. As the main dipeptide-bound amino acids identified in urine were glycine and cystine we hypothesized that they are derived from cys-gly, a break-down product of GSH (γ-glutamyl-cysteinyl-glycine). We therefore analyzed spot urine samples for cysteinyl-glycine by HPLC with a thiol-specific derivatization procedure. As shown in Fig. 1, excretion of the dipeptide cys-gly was increased 18-fold in male *Pept2*$^{-/-}$ animals and 5-fold in female *Pept2*$^{-/-}$ mice.

GSH Concentration in Kidney Tissue and Expression Level of Genes Involved in GSH Metabolism

As the excretion of the GSH breakdown product cys-gly was drastically increased and levels of glycine and cysteine were lower in kidney tissue of transporter-deficient animals, we hypothesized that the concentrations of GSH in the kidney might also be altered in *Pept2*$^{-/-}$ animals due to an impaired supply of substrates for GSH synthesis. Analysis of GSH in kidney tissue by HPLC with thiol-specific derivatization, however, revealed no significant differences between *Pept2*$^{+/+}$ (4.19 ± 0.24 μmol/g tissue) and *Pept2*$^{-/-}$ (3.87 ± 0.11 μmol/g tissue) animals. Expression of enzymes involved in GSH metabolism was studied at mRNA levels by qPCR to assess whether changes in enzymes needed for GSH synthesis could compensate for a lower supply of substrates, yet no significant changes in transcript levels were observed for any of the selected enzymes (Table 4).

DISCUSSION

We here provide data of a comprehensive analysis of changes in kidney tissue samples of *Pept2*$^{-/-}$ mice that may help to identify metabolic perturbations that do not lead to an obvious phenotype because of biological compensatory mechanisms. Profiling technologies employed to identify changes in kidney tissues at the mRNA, protein, and metabolite levels revealed numerous subtle but significant changes at the mRNA, protein, and metabolite levels that may for the first time shed some light on the prime role of the peptide transporter PEPT2 in renal tubules.

A classification of regulated gene products at mRNA and protein levels according to the gene ontology (GO) classification for biological processes provided predominantly targets of kidney epithelial cell metabolism that changed by loss of PEPT2. Underrepresented are processes like regulation of transcription, signal transduction, and cell communication. As reported by others (2, 8, 17), we also found very little concordance between changes in mRNA and the corresponding protein levels. Gstm1 was the only gene product with a similar regulation at mRNA and protein level. Yet differentially expressed mRNAs and proteins all fell into the same categories of the GO classification. Enzymes of amino acid metabolism were particularly overrepresented within the groups of differentially expressed mRNAs and proteins (Table S. 2). In addition, a number of enzymes of lipid and fatty acid metabolism (Table S. 3), such as carnitine-palmitoyltransferase 2 (*Cpt2*), long chain acyl CoA synthetase (*Acsl1*), acyl-CoA-thioesterase 3 (*Acot3*), and acetyl-CoA acyltransferase 1A and 1B (*Acaa1a*, *Acaa1b*), were found regulated. Although the changes observed for the latter enzymes suggested an increase in fatty acid beta oxidation in *Pept2*$^{-/-}$ kidney tissues, no corresponding changes at the metabolite levels (i.e., fatty acids) could be observed. Far more consistent, however, were alterations in amino acid metabolism in which not only mRNA and protein entities changed but also metabolites, in particular various amino acids and their derivatives (Table 2). Pathway analysis

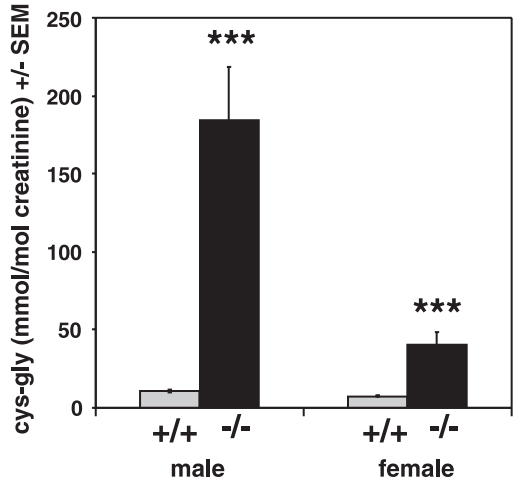

Fig. 1. Urinary cysteinyl-glycine (cys-gly). Urinary concentration of cys-gly in directly collected spontaneous urine of male and female animals; $n = 10$ per sex and genotype. Data were analyzed by double-sided, unpaired Student's *t*-test for differences between genotypes. Significant differences between knockout and wild-type animals are marked with asterisks (***$P < 0.001$).

Table 4. *Expression of selected genes involved in glutathione metabolism*

Gene Symbol Accession No.	Description	MNE +/+	MNE −/−	Fold Change −/− vs. +/+
Gclm NM_145953	glutamylcysteine ligase modifier subunit	0.583±0.067	0.817±0.133	1.40
Gclc NM_010295	glutamylcysteine ligase catalytic subunit	0.634±0.101	0.650±0.110	1.03
Gss NM_008180	glutathione synthetase	1.16±0.10	1.07±0.10	0.92
Ggt1 NM_008116	γ-glutamyl-transferase	11.3±1.8	9.45±1.02	0.83
Gsr NM_010344	glutathione reductase 1	0.449±0.092	0.739±0.092	1.65
Cth NM_145953	cystathionine gamma-lyase	0.585±0.106	0.922±0.161	1.58

mRNA expression was analyzed by quantitative real-time RT-PCR (qPCR) in $n = 5$ kidney RNA samples per genotype and diet. Mean normalized expression (MNE) values ± SE were calculated with Q-Gene. The geometric mean of crossing point values of 3 housekeeping gene was calculated, and this best-keeper index was applied for normalization. MNE values were tested by Kruskal-Wallis test for differences between genotypes. No significant difference in expression between WT and KO animals was detected.

tools such as KEGG (http://www.genome.jp/kegg/), Brenda (Cologne University Bioinformatics Centre, Germany; release 5.2 http://www.brenda.uni-koeln.de/), and MetaCore (GeneGo, St. Joseph, MI; http://www.genego.com/) were used to compile Fig. 2, which is a schematic representation of metabolic pathways and their links for which corresponding changes in any of the biological entities could be identified in kidney tissues of transporter-deficient mice. It becomes obvious that the amino

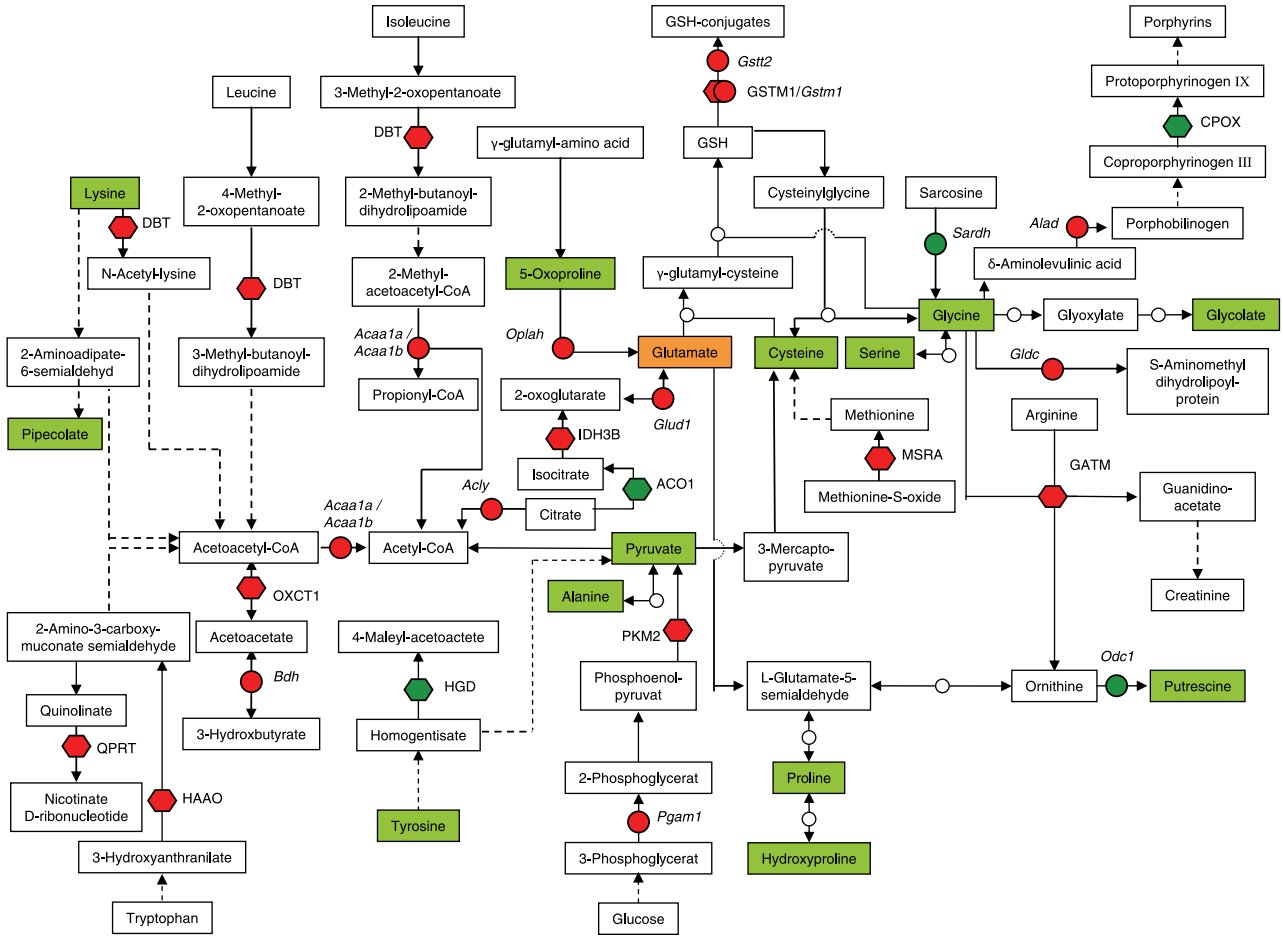

Fig. 2. Metabolic pathways affected by loss of PEPT2 in kidney tissues. Changes at the mRNA, protein, and/or metabolite level that could be assigned to metabolic pathways are depicted. Differentially expressed gene products (mRNA or protein) are denoted with the gene symbol for Acaa1a, acetyl-coenzyme A acyltransferase 1A; Acaa1b, 3-ketoacyl-CoA thiolase B; Acly, ATP citrate lyase; Aco1, aconitate hydratase; Alad, delta-aminolevulinate dehydratase; Bdh, 3-hydroxybutyrate dehydrogenase; Cpox, coproporphyrinogen oxidase; Dbt, dihydrolipoamide transacylase precursor; Gatm, glycine amidinotransferase; Gldc, glycine decarboxylase; Glud1, glutamate dehydrogenase 1; Gstm1, glutathione S-transferase mu 1; Gstt2, glutathione S-transferase theta 2; Haao, 3-hydroxyantranilate 3.4-dioxygenase; Hgd, homogentisate dioxigenase; Idh3b, isocitrate dehydrogenase 3 (NAD+) beta; Msra, methionine sulfoxide reductase A; Odc1, mouse ornithine decarboxylase gene; Oplah, 5-oxoprolinase; Oxct1, 3-oxoacid CoA transferase; Pgam1, phosphoglycerate mutase 1; Pkm2, pyruvate kinase M2 isozyme; Qprt, quinolinate phosphoribosyltransferase; Sardh, sarcosine dehydrogenase. Orange boxes, metabolites with increased concentration in *Pept2*$^{-/-}$ mice; green boxes, metabolites with lower concentration in *Pept2*$^{-/-}$ mice; white boxes, metabolites with no change in concentration between genotypes; red circles, elevated mRNA level in *Pept2*$^{-/-}$ mice; green circles, decreased mRNA level in *Pept2*$^{-/-}$ mice; red hexagons, elevated protein concentration in *Pept2*$^{-/-}$ mice; green hexagons, decreased protein concentration in *Pept2*$^{-/-}$ mice; solid arrows, direct reaction within the pathway; dotted arrows, intermediary metabolites and reactions omitted.

acids glutamate, cysteine, and glycine, as well as 5-oxoproline, are in prominent positions, and both transcripts and proteins associated with their metabolism were found regulated. These amino acids are all constituents of GSH, and this suggested that tubular GSH handling might be impaired in *Pept2*$^{-/-}$ mice. The second line of evidence for alterations in GSH metabolism comes from urine analysis. Urine samples contained increased concentrations of cys-gly, and when amino acid levels in urine were analyzed after hydrolysis by the dipeptidase, again only glycine and cystine concentrations increased (Fig. 1, Table 3). These data provided evidence that the most prominent dipeptides that can be found in kidney tubular fluids are those consisting of glycine and cysteine residues and that the only one identified that shows drastically increased excretion rates in *Pept2*$^{-/-}$ mice is cys-gly. The increased excretion of amino acids and particular of cys-gly by the transporter-deficient animals did not result from increased plasma levels, and thus a higher tubular load since plasma levels of amino acids and cys-gly did not differ between *Pept2*$^{+/+}$ and *Pept2*$^{-/-}$ animals (data not shown). Urinary cys-gly is most likely a product of the break-down of GSH as extracellular degradation of GSH by *Ggt1* leads to cys-gly and γ-glutamyl-amino acids (9). GSH is found in plasma with mean concentrations of 10 μM and reaches after glomerular filtration the tubular system in which also a GSH secretion takes place (19). In the tubule, GSH is then cleaved by *Ggt1* into cys-gly and a γ-glutamyl-amino acid. It can be anticipated that cys-gly is normally cleaved further by membrane-bound dipeptidases and that the free amino acids are then reabsorbed for resynthesis of GSH in tubular cells. How the γ-glutamyl-amino acids are taken up into epithelial cells is not understood as yet, but γ-glutamyl-amino acids can be metabolized within the cell by γ-glutamyl-cyclotransferase (*Ggc*) to oxoproline, which can be converted to glutamate by oxoprolinase (*Oplah*). Although γ-glutamyl-amino acids are not transported by PEPT2 (unpublished observations), we observed lower levels of oxoproline and increased mRNA levels of oxoprolinase in the transporter-deficient animals.

An alternative and most likely more important route for reabsorption of the GSH break-down products is the uptake of cys-gly via PEPT2 followed by intracellular hydrolysis to yield glycine and cysteine. Cys-gly has been shown to be a good substrate for PEPT2 and can be used efficiently for GSH synthesis (11). The 18-fold increase in renal loss of cys-gly in male *Pept2*$^{-/-}$ mice suggests that the uptake of the intact dipeptide is important for renal scavenging of the GSH constituents. It is interesting to note that two intracellular peptidases (*Napsa, Xpnpep*) and a cytosolic dipeptidase (*Cndp2*) were identified as regulated in expression level in *Pept2*$^{-/-}$ mice, which suggests that they could be involved in hydrolysis of cys-gly after its uptake into tubular cells or intracellular protein hydrolysis if cellular free amino acid levels are low. GSH is resynthesized in renal tubular cells from glutamate, cysteine, and glycine via γ-glutamyl-cysteine by glutamylcysteine synthetase (consisting of the subunits *Gclm* and *Gclc*) and *Gss*. Figure 3 gives a schematic view of renal GSH metabolism and the proposed involvement of PEPT2. For assessing whether these enzymes needed for GSH resynthesis showed any changes in expression levels in kidney tissues, we performed qPCR amplifications of mRNA, but this did not reveal any significant adaptations in transcript levels. Surprisingly, GSH levels determined by HPLC with thiol-specific derivatization also revealed no differences between control animals and transporter-deficient animals despite lower cellular concentrations of the precursor amino acids. These unchanged GSH levels, however, may be explained best by an increased uptake of GSH from the blood across the basolateral membrane of tubular cells. It has been suggested that the sodium-dicarboxylate transporter 2 (Sdct-2) and the organic anion transporters 1 (Oat1) and 3 (Oat3) mediate basolateral GSH uptake (19), and our cDNA microarray analysis indeed revealed increased mRNA levels for Oat3 as a putative GSH import system.

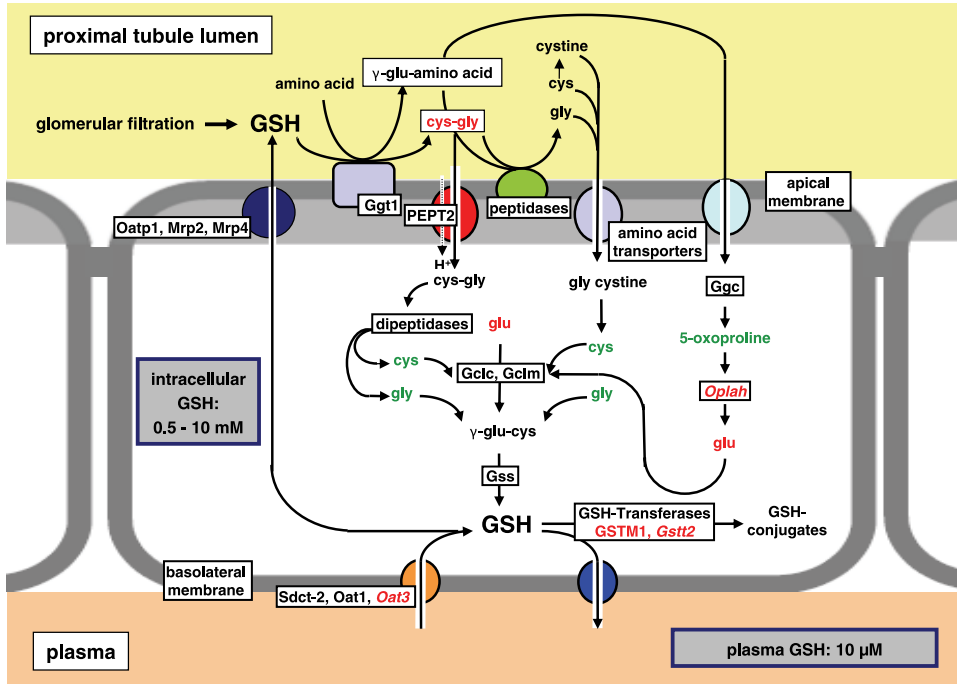

Fig. 3. Schema of GSH metabolism in epithelial cells of the proximal tubule. GSH is degraded and resynthesized in proximal tubular cells via the γ-glutamyl-cycle. By reabsorption of cys-gly, PEPT2 could deliver substrates for resynthesis of GSH. Enzymes, transporters, and metabolites with increased expression or concentration in the transporter deficient animals are labeled in red, and entities with decreased expression or concentration are labeled in green. Gclc, glutamylcysteine ligase catalytic subunit; Gclm, glutamylcysteine ligase modifier subunit; Ggc, γ-glutamyl-cyclotransferase; Ggt1, γ-glutamyl-transferase; Gss, glutathione synthetase; Gstm1, glutathione S-transferase mu1; Gstt2, glutathione S-transferase theta 2; Mrp2, multidrug resistance-associated protein 2; Mrp4, multidrug resistance-associated protein 4; Oat1, organic anion transporter 1; Oat3, organic anion transporter 3; Oatp1, organic anion transporting polypeptide 1; Oplah, 5-oxoprolinase; Sdct-2, sodium-dicarboxylate transporter 2.

Despite the lack of changes in tissue GSH levels, an upregulation of the glutathione transferases *Gstt2* at the mRNA level and an upregulation of Gstm1 at mRNA and protein levels suggest that the GSH turnover of renal cells may be affected not only by the identified lower levels of the precursor amino acids in *Pept2*$^{-/-}$ mice but also by its use for conjugation and detoxification employing the glutathione transferases.

Other changes in metabolic pathways of amino acids in tubular cells as based on the transcriptome, proteome, and metabolite analysis data suggest that, for example, less ornithine is used for polyamine synthesis involving the identified *Odc1* enzyme that could lead to the decreased levels of putrescine found. Identified transcripts for enzymes surrounding altered glutamate, alanine, and pyruvate levels suggest that nitrogen shuttling may also be altered. Two regulated enzymes of the pathway that leads from glycine via δ-aminolevulinic acid to porphyrins (*Alad* and *CPOX*) suggest impairments in this metabolic route, and in this context it is interesting to note that δ-aminolevulinic acid has been shown to be a good substrate of the peptide transporter PEPT2. The question of whether its renal uptake and metabolism is affected in *Pept2*$^{-/-}$ mice needs further studies.

In summary, kidneys of mice that lack the renal high affinity type peptide transporter PEPT2 and that do not show any prominent phenotypic alterations display, when profiled by combined DNA microarray, proteome, and metabolite analysis techniques, numerous subtle yet significant changes in cell metabolism and renal excretion of amino acids and peptides. Although every profiling technique used here has its limitations in terms of sensitivity of detection (proteome and metabolite profiling) or interpretation of biological relevance (mRNA level), their combination allowed us for the first time to identify alterations in renal handling of peptides, amino acids, and derivatives in the transporter-deficient animals. From our study it may be concluded that the prime function of PEPT2 in the S2/S3 segment of the tubule is the reabsorption of cys-gly as the prime breakdown product of extracellular GSH-hydrolysis. Cys-gly is found in plasma in concentrations of 15–70 μM and is filtered in the glomerulum to reach tubular cells (3, 16, 37). Cys-gly concentrations in human urine are $<$10 μM (22, 27), indicating an efficient reabsorption in renal tubules. Filtered plasma GSH and GSH secreted into the tubule are hydrolyzed by membrane-bound *Ggt1* to yield cys-gly, which then is taken up together with the filtered cys-gly into renal tubular cells via PEPT2. The drastically increased excretion of cys-gly in the transporter-deficient animals demonstrates the role of PEPT2 in reabsorption of substrates for intracellular GSH resynthesis. Despite any detectable changes in cellular free GSH levels, a variety of metabolic pathways surrounding glycine, cysteine, and glutamate as the precursor amino acids for GSH resynthesis showed alterations of metabolite concentrations as well as changes in mRNA and/or protein levels of enzymes linked to their metabolisms. Although the markedly reduced tubular uptake capacity for cys-gly in *Pept2*$^{-/-}$ mice is obviously compensated for without functional impairments in the kidney, it could be that conditions with an increased demand for GSH such as increased burden of reactive oxygen species may cause pathophysiology in these mice.

ACKNOWLEDGMENTS

Present addresses: I. Rubio-Aliaga, Institute of Experimental Genetics, GSF, Neuherberg, Germany; A. Drobyshev, Engelhardt Institute of Molecular Biology, 119991 Moscow, Russia.

GRANTS

This work was supported in part by Else-Kroener-Fresenius-Stiftung Grant 1512/282 72-5 and the European FP6 project EUGINDAT.

REFERENCES

1. **Adibi SA.** Renal assimilation of oligopeptides: physiological mechanisms and metabolic importance. *Am J Physiol Endocrinol Metab* 272: E723–E736, 1997.
2. **Anderson L, Seilhamer J.** A comparison of selected mRNA and protein abundances in human liver. *Electrophoresis* 18: 533–537, 1997.
3. **Badiou S, Bellet H, Lehmann S, Cristol JP, Jaber S.** Elevated plasma cysteinylglycine levels caused by cilastatin-associated antibiotic treatment. *Clin Chem Lab Med* 43: 332–334, 2005.
4. **Benjamini Y, Hochberg Y.** Controlling the false discovery rate: a practical and powerful approach to multiple testing. *J Royal Stat Soc B* 57: 289–300, 1995.
5. **Boll M, Herget M, Wagener M, Weber WM, Markovich D, Biber J, Clauss W, Murer H, Daniel H.** Expression cloning and functional characterization of the kidney cortex high-affinity proton-coupled peptide transporter. *Proc Natl Acad Sci USA* 93: 284–289, 1996.
6. **Boll M, Markovich D, Weber WM, Korte H, Daniel H, Murer H.** Expression cloning of a cDNA from rabbit small intestine related to proton-coupled transport of peptides, beta-lactam antibiotics and ACE-inhibitors. *Pflügers Arch* 429: 146–149, 1994.
7. **Botka CW, Wittig TW, Graul RC, Nielsen CU, Higaka K, Amidon GL, Sadee W.** Human proton/oligopeptide transporter (POT) genes: identification of putative human genes using bioinformatics. *AAPS PharmSci* 2: E16, 2000.
8. **Chen G, Gharib TG, Huang CC, Taylor JM, Misek DE, Kardia SL, Giordano TJ, Iannettoni MD, Orringer MB, Hanash SM, Beer DG.** Discordant protein and mRNA expression in lung adenocarcinomas. *Mol Cell Proteomics* 1: 304–313, 2002.
9. **Curthoys NP.** Role of gamma-glutamyltranspeptidase in the renal metabolism of glutathione. *Miner Electrolyte Metab* 9: 236–245, 1983.
10. **Delmar P, Robin S, Daudin JJ.** VarMixt: efficient variance modelling for the differential analysis of replicated gene expression data. *Bioinformatics* 21: 502–508, 2005.
11. **Dringen R, Hamprecht B, Broer S.** The peptide transporter PepT2 mediates the uptake of the glutathione precursor CysGly in astroglia-rich primary cultures. *J Neurochem* 71: 388–393, 1998.
12. **Fei YJ, Ganapathy V, Leibach FH.** Molecular and structural features of the proton-coupled oligopeptide transporter superfamily. *Prog Nucleic Acid Res Mol Biol* 58: 239–261, 1998.
13. **Fei YJ, Kanai Y, Nussberger S, Ganapathy V, Leibach FH, Romero MF, Singh SK, Boron WF, Hediger MA.** Expression cloning of a mammalian proton-coupled oligopeptide transporter. *Nature* 368: 563–566, 1994.
14. **Frey IM, Rubio-Aliaga I, Klempt M, Wolf E, Daniel H.** Phenotype analysis of mice deficient in the peptide transporter PEPT2 in response to alterations in dietary protein intake. *Pflügers Arch* 452: 300–306, 2006.
15. **Fuchs D, Erhard P, Rimbach G, Daniel H, Wenzel U.** Genistein blocks homocysteine-induced alterations in the proteome of human endothelial cells. *Proteomics* 5: 2808–2818, 2005.
16. **Garibotto G, Sofia A, Saffioti S, Russo R, Deferrari G, Rossi D, Verzola D, Gandolfo MT, Sala MR.** Interorgan exchange of aminothiols in humans. *Am J Physiol Endocrinol Metab* 284: E757–E763, 2003.
17. **Gygi SP, Rochon Y, Franza BR, Aebersold R.** Correlation between protein and mRNA abundance in yeast. *Mol Cell Biol* 19: 1720–1730, 1999.
18. **Hegde P, Qi R, Abernathy K, Gay C, Dharap S, Gaspard R, Hughes JE, Snesrud E, Lee N, Quackenbush J.** A concise guide to cDNA microarray analysis. *Biotechniques* 29: 548–550, 552–544, 556 passim, 2000.
19. **Lash LH.** Role of glutathione transport processes in kidney function. *Toxicol Appl Pharmacol* 204: 329–342, 2005.
20. **Lin CJ, Smith DE.** Glycylsarcosine uptake in rabbit renal brush border membrane vesicles isolated from outer cortex or outer medulla: evidence

for heterogeneous distribution of oligopeptide transporters. *AAPS PharmSci* 1: E1, 1999.
21. **Liu W, Liang R, Ramamoorthy S, Fei YJ, Ganapathy ME, Hediger MA, Ganapathy V, Leibach FH.** Molecular cloning of PEPT 2, a new member of the H+/peptide cotransporter family, from human kidney. *Biochim Biophys Acta* 1235: 461–466, 1995.
22. **Lochman P, Adam T, Friedecky D, Hlidkova E, Skopkova Z.** High-throughput capillary electrophoretic method for determination of total aminothiols in plasma and urine. *Electrophoresis* 24: 1200–1207, 2003.
23. **Meissner B, Boll M, Daniel H, Baumeister R.** Deletion of the intestinal peptide transporter affects insulin and TOR signaling in Caenorhabditis elegans. *J Biol Chem* 279: 36739–36745, 2004.
24. **Muller PY, Janovjak H, Miserez AR, Dobbie Z.** Processing of gene expression data generated by quantitative real-time RT-PCR. *Biotechniques* 32: 1372–1374, 1376, 1378–1379, 2002.
25. **Ocheltree SM, Shen H, Hu Y, Keep RF, Smith DE.** Role and relevance of peptide transporter 2 (PEPT2) in the kidney and choroid plexus: in vivo studies with glycylsarcosine in wild-type and PEPT2 knockout mice. *J Pharmacol Exp Ther* 315: 240–247, 2005.
26. **Palacin M, Estevez R, Bertran J, Zorzano A.** Molecular biology of mammalian plasma membrane amino acid transporters. *Physiol Rev* 78: 969–1054, 1998.
27. **Pastore A, Piemonte F, Locatelli M, Lo Russo A, Gaeta LM, Tozzi G, Federici G.** Determination of blood total, reduced, and oxidized glutathione in pediatric subjects. *Clin Chem* 47: 1467–1469, 2001.
28. **Pattyn F, Speleman F, De Paepe A, Vandesompele J.** RTPrimerDB: the real-time PCR primer and probe database. *Nucleic Acids Res* 31: 122–123, 2003.
29. **Pfaffl MW, Tichopad A, Prgomet C, Neuvians TP.** Determination of stable housekeeping genes, differentially regulated target genes and sample integrity: BestKeeper–Excel-based tool using pair-wise correlations. *Biotechnol Lett* 26: 509–515, 2004.
30. **Rubio-Aliaga I, Daniel H.** Mammalian peptide transporters as targets for drug delivery. *Trends Pharmacol Sci* 23: 434–440, 2002.
31. **Rubio-Aliaga I, Frey I, Boll M, Groneberg DA, Eichinger HM, Balling R, Daniel H.** Targeted disruption of the peptide transporter Pept2 gene in mice defines its physiological role in the kidney. *Mol Cell Biol* 23: 3247–3252, 2003.
32. **Ruhl A, Hoppe S, Frey I, Daniel H, Schemann M.** Functional expression of the peptide transporter PEPT2 in the mammalian enteric nervous system. *J Comp Neurol* 490: 1–11, 2005.
33. **Sakata K, Yamashita T, Maeda M, Moriyama Y, Shimada S, Tohyama M.** Cloning of a lymphatic peptide/histidine transporter. *Biochem J* 356: 53–60, 2001.
34. **Seltmann M, Horsch M, Drobyshev A, Chen Y, de Angelis MH, Beckers J.** Assessment of a systematic expression profiling approach in ENU-induced mouse mutant lines. *Mamm Genome* 16: 1–10, 2005.
35. **Shen H, Smith DE, Keep RF, Xiang J, Brosius FC 3rd.** Targeted disruption of the PEPT2 gene markedly reduces dipeptide uptake in choroid plexus. *J Biol Chem* 278: 4786–4791, 2003.
36. **Steiner HY, Naider F, Becker JM.** The PTR family: a new group of peptide transporters. *Mol Microbiol* 16: 825–834, 1995.
37. **Suliman ME, Divino Filho JC, Barany P, Anderstam B, Lindholm B, Bergstrom J.** Effects of high-dose folic acid and pyridoxine on plasma and erythrocyte sulfur amino acids in hemodialysis patients. *J Am Soc Nephrol* 10: 1287–1296, 1999.
38. **Wang X, Seed B.** A PCR primer bank for quantitative gene expression analysis. *Nucleic Acids Res* 31: e154, 2003.
39. **Weckwerth W, Loureiro ME, Wenzel K, Fiehn O.** Differential metabolic networks unravel the effects of silent plant phenotypes. *Proc Natl Acad Sci USA* 101: 7809–7814, 2004.
40. **Weckwerth W, Wenzel K, Fiehn O.** Process for the integrated extraction, identification and quantification of metabolites, proteins and RNA to reveal their co-regulation in biochemical networks. *Proteomics* 4: 78–83, 2004.
41. **Yamashita T, Shimada S, Guo W, Sato K, Kohmura E, Hayakawa T, Takagi T, Tohyama M.** Cloning and functional expression of a brain peptide/histidine transporter. *J Biol Chem* 272: 10205–10211, 1997.
42. **Yang YH, Dudoit S, Luu P, Lin DM, Peng V, Ngai J, Speed TP.** Normalization for cDNA microarray data: a robust composite method addressing single and multiple slide systematic variation. *Nucleic Acids Res* 30: e15, 2002.